CONF-961017--13

Attachment A

Return with Camera-Ready Manuscript

Cover Information for ASM Technical Papers
(For inclusion in the ASM Proceedings)

In order to ensure that the correct title, author names, and affiliations appear on the cover and title page of your paper, please provide the information requested below.

Type the exact title of the paper, the author(s), and affiliation(s)—include city and state—in upper and lower case (For example: New High-Temperature Alloys, J. Jones, ABC Inc., Cleveland, OH). ASM will have the copy set in bold headline type for placement on the first page of the paper. Do not include author's title (Prof., Dr.), position (president, research engineer), or degrees (Ph.D., M.E.).

Paper Title (upper and lower cases)

Reaction Synthesis and Processing of Nickel and Iron Aluminides

Author(s) (upper and lower case)	Affiliation(s) (city & state) (upper and lower case)
1. Seetharama C. Deevi	1. Research Center Philip Morris U.S.A. Richmond, Virginia 23234
2. Vinod K. Sikka	2. Metals and Ceramics Division Oak Ridge National Laboratory Oak Ridge, Tennessee 37831-6083
3.	3.
4.	4.
5.	5.

Conference: 1996 ASM Materials Week
Int. Symp. on Nickel and Iron Aluminides: Processing, Properties, and Applications

Note: Materials submitted for publication will not be returned unless requested by the author.

DISCLAIMER

Abstract

Composites of nickel and iron aluminides were obtained by hot-pressing and hot-extrusion of a blended mixture of nickel and aluminum or iron and aluminum with ceramic phases such as TiC, ZrO_2, and Al_2O_3. Aluminides were analyzed by X-ray diffraction technique to determine the phase structures of the materials, and optical and scanning electron microscopic techniques were used to determine the grain sizes of the aluminides and dispersion of ceramics. Tensile properties such as 0.2% yield strength, ultimate tensile strength, total elongation, and reduction in area were measured on button-head and sheet specimens of nickel and iron aluminides and their composites at room and elevated temperatures in air at a strain rate of $1.2 \times 10^{-3}s^{-1}$. Tensile properties of Fe-8 wt % Al alloys obtained by partial mechanical alloying followed by combustion synthesis compare extremely well with the oxide-dispersed alloys of iron. Iron aluminides of FeAl and their composites, based on Fe-24 wt % Al obtained by hot-pressing of iron and aluminum powders with or without ceramic phases, exhibited full densities and uniform grain sizes. The 0.2% yield strengths, tensile strengths, and tensile elongations of FeAl and their composites, based on hot-pressing of elemental powders, exhibited excellent mechanical properties as compared to the mechanical properties of FeAl alloys obtained by hot-extrusion of water-atomized powders. Iron aluminides were also obtained by hot-extrusion of iron and aluminum powders at extrusion temperatures of 950, 1000, and 1100°C.

DURING THE LAST DECADE, synthesis and processing of materials by the combustion synthesis technique has been extended to a wide variety of materials by several reseachers throughout the world. The technique is also referred to as self-propagating high-temperature synthesis, thermal explosion mode of combustion synthesis, and as-reaction synthesis. Several papers and reviews describe the fundamentals, applications, and limitations of the technique (1-4). While the energy savings and purity of the products have long been realized, the technique's main limitation has been the porous nature of the product. Application of pressure is shown to reduce the porosity, and, in some cases, innovative densification techniques led to fully dense materials (5-11). Even with the limitations of the original technique, the principles have been extended to obtain a wide variety of interesting composites based on thermite reactions (12-14). Research conducted at the Oak Ridge National Laboratory (ORNL) on the application of reaction-synthesis principles to the melt stock allowed melting of over 30,000 kg of nickel and iron aluminides for a variety of industrial applications, and allowed realization of the intermetallic properties known for over four decades or longer (15-19). We briefly describe the attributes of nickel and iron aluminides prior to discussing the extension of reaction-synthesis principles to intermetallics.

Intermetallic compounds based on iron and nickel aluminides possess high-melting points, simple ordered crystal structures, low densities (10 to 25% lower than superalloys), and interesting mechanical properties. They possess sufficiently high concentrations of aluminum in the range of 13 to 32 wt % to form continuous, fully adherent alumina layers on the surface when exposed to air or oxygen atmospheres. Alumina layers formed on the surfaces of aluminides provide excellent oxidation and carburization resistances up to 1100°C or higher. Recent advances in alloying design involving small additions of boron to an off-stoichiometric Ni_3Al resulted in a tensile ductility of 40 to 50%. However, NiAl still exhibits very low ductility at room temperature and lacks high-temperature strength for monolithic applications. Nickel aluminide based on Ni_3Al exhibits excellent wear resistance, and wear resistance of Ni_3Al increases

Seetharama C. Deevi

with increasing temperature by two to three orders of magnitude. Also, the cavitation erosion resistance of Ni_3Al is superior to many of the currently used materials. The attributes discussed above make intermetallics based on Ni_3Al and NiAl suitable for a variety of high-temperature powder-metallurgical and coating applications to protect the substrate materials against oxidation, corrosion, erosion, and wear in specific environments (20-22).

On the other hand, the ductility of iron aluminides are lower than Ni_3Al, and iron aluminides are susceptible to hydrogen embrittlement. The density of iron aluminides is lower than many stainless steels and, thus, offer better strength to weight ratio. Iron aluminides are resistant to sulfidation in H_2S and SO_2 gases, and their sulfidation resistance is better than any other iron- or nickel-based alloys. Unlike many commercial metallic materials, iron aluminides exhibit high-electrical resistivity (50 to 100% higher than commercial heating elements) and, thus, making them ideally suited for home- and industrial-heating applications. They also have good corrosion resistance in many aqueous environments and can be deposited as coatings for chemical industry (23-26).

The intermetallic alloys were developed at the Oak Ridge National Laboratory (ORNL) as cast and wrought products; therefore, a wide range of nickel- and iron-aluminide compositions were excluded due to the solidification porosity and other incompatibilities with the processing methods. Powder-metallurgical-processing techniques such as mechanical alloying, hot-pressing, and hot-extrusion offer a considerable flexibility in exploiting the unique attributes of intermetallics and their composites. A simple application of pressure during the combustion wave propagation may not lead to full densification since an intermetallic may have a very limited ductility at high temperatures, and application of pressure can crack the sample. Also, the temperature is quickly lost to the dies. On the other hand, densification can be carried out by hot-forging of combustion-synthesized samples as long as the porous intermetallic did not undergo any oxidation. Densification can also be achieved by hot-pressing and hot-extrusion of intermetallic powders.

In this paper, we briefly describe the principles of reaction synthesis, and show that intermetallics can be obtained by the use of appropriate elemental powders. Dense intermetallics based on iron aluminides were obtained by mechanical alloying followed by combustion synthesis, hot-pressing, and hot-extrusion of elemental powders. Optical microscopic techniques were employed to determine grain sizes and the uniformity of the phases, and mechanical properties were obtained to determine the strengths and elongations of iron aluminides. Properties of dense nickel aluminides obtained by hot-pressing of elemental powders were also discussed. Reaction-synthesis principles have also been extended to obtain plasma-spray coatings of nickel aluminides, and to melting and casting of intermetallics.

Continue text reading pages below this line

Reaction Synthesis

The reaction-synthesis technique allows the synthesis of materials with large negative heats of formation with minimal application of external heat. This technique has been widely used with powdered compacts of elemental mixtures in which ignition of an upper surface of the compact leads to a strong exothermic reaction (as with a mixture of nickel and aluminum). The exothermic reaction liberates sufficient heat to raise the temperature of the adjacent layer of reactants so that the reaction becomes self-sustained. This technique is widely known as self-propagating high-temperature synthesis or combustion synthesis and was extensively investigated in the former Soviet Union (5-8). The reaction-synthesis technique is based primarily on thermodynamic criteria that formation of the products must be accompanied by lowering of Gibbs free energy and release of a significant amount of energy. In general, the formation of nickel and iron aluminides is an exothermic process (see Table I), and the heat of reaction varies depending on the ratio of transition metal to aluminum. This can be seen from Figure 1 that the heat released in the case of Ni-Al is based on the ratio of Ni/Al, and the adiabatic combustion temperatures vary accordingly). Temperature rise due to the exothermic reaction is also strongly dependent on the initial temperature of the components. Thermodynamic principles have been used to calculate the maximum attainable temperatures during the formation of aluminides due to the reaction between nickel or iron and aluminum.

Table I. Heats of formation, aluminum content, and melting points of selected intermetallics

Intermetallic	Heat of formation ΔHf_{298} (K cal/mole)	Weight percent of aluminum	Melting point (°C)
Ni_3Al	-36.6 ± 1.2	13.28	1395
NiAl	-28.3 ± 1.2	31.49	1639
Ni_2Al_3	-67.5 ± 4.0	40.81	1133
$NiAl_3$	-36.0 ± 2.0	57.96	854
Fe_3Al	-16.648	13.87	1502
FeAl	-12.0	32.57	1215
$FeAl_2$	-18.9	49.1	1164
Fe_2Al_5	-34.3	54.70	1171

An enthalpy balance based on the heat of reaction and the initial temperature will provide an insight on the maximum attainable temperature and whether the intermetallic would be in liquid or solid state, as in the following equations:

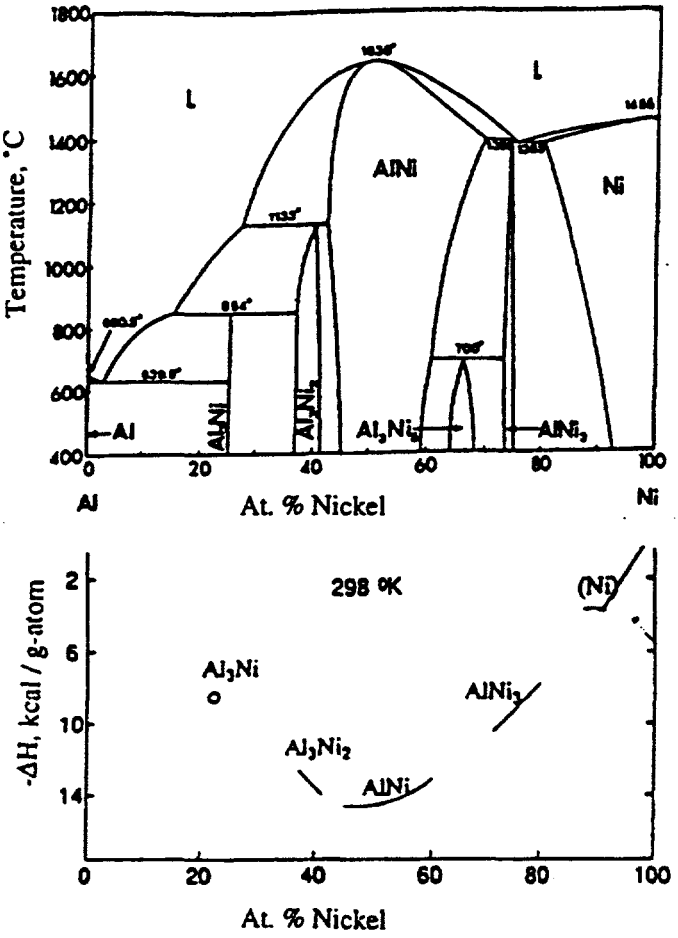

Figure 1 - Phase diagram of the Ni-Al system, and the heats of formation associated with nickel-aluminide phases.

$$\Delta H^{r}_{T_0} = \int_{T_0}^{T_{ad}} CpdT \qquad (1)$$

and

$$\Delta H^{r}_{T_0} = \int_{T_0}^{T_m} CpdT + f\Delta H_m \ , \qquad (2)$$

where

$\Delta H^{r}_{T_0}$ = the enthalpy of reaction at T_0,

Cp = the heat capacities of the product.

Equation (2) above takes into consideration the phase transformation accompanying melting of the product and its latent heat of fusion, ΔH_m.

If the product undergoes melting below the adiabatic temperature, T_{ad}, the fraction in molten condition, f, can be calculated from Eq. (2). Equations (1) and (2) above assume adiabatic conditions, and T_{ad} in Eq. (1) provides an upper limit for the temperature. A simple calculation of T_{ad}, based on Eq. (1), suggests that the maximum temperatures are close to the melting point, and molten product may appear only in the case of NiAl. With an initial temperature of 660 to 800°C, the enthalpy balance of Eq. (2) indicates that the product will be in the liquid state in the case of nickel and iron aluminides.

The nature of the reactants and their composition will determine the product formed and also the amount of energy released. Also parameters such as interfacial contact area between nickel and aluminum, aluminum content, and particle size determine the fraction of the molten product (11-14).

Simultaneous Reaction Synthesis and Densification by Hot-Pressing of Elemental Powders

In this technique, elemental powders of the intermetallic of interest were blended in a V-blender for 24 h with 1.25-cm alumina or zirconia balls, and the blended powder was loaded in a 5-cm-diam graphite die. To obtain an intermetallic composite, ceramic reinforcement of appropriate quantity was added to the elemental powders prior to blending. A small amount of uniaxial pressure was applied to the graphite punches through the ram, and was evacuated to 10^{-5} torr before raising the temperature to a maxiumum of 1100 to 1200°C and a pressure of 35 to 50 MPa. Even though the applied pressure is uniaxial in nature on the powders, powders experience a radial pressure due to the constraint of the die wall. The temperature, vacuum, and the movement of the ram were noted to determine the rate of densification and to gain insight whether the densification is associated with the melting of aluminum.

Densification process was monitored by noting down the ram travel versus applied pressure on the powders, and the temperature of the graphite die. As can be seen from Figures 2 and 3, a significant ram travel occurred around the melting point of aluminum, suggesting that the intermetallic formation and densification occur almost simultaneously. Interestingly, an upward ram travel was noted almost immediately after crossing the melting point of aluminum, and this upward ram travel could be attributed to the changes in molar-volume differences between elemental powders and the intermetallic. This was indeed noted in a variety of systems during the combustion synthesis of ceramics such as carbides of titanium, zirconium, and hafnium; nitrides of titanium, zirconium, and hafnium; silicides of molybdenum and titanium, and intermetallics such as NiAl (5).

Microstructures of hot-pressed intermetallics and their composites attained near-full density (27) and exhibited fine-grain sizes on the order of 20 to 30 μm (see Table II). Figure 4 shows the microstructures of Ni3Al with 2 and 4 wt % of alumina at a magnification of 100×. Vickers microhardnesses of hot-pressed samples shown in Figure 5 indicate that the microhardnesses of hot-pressed samples are higher than the microhardness of cast Ni3Al, and are in the range of 280 to 290 kg/mm^2. Hot-pressing of elemental powders of composition corresponding to Fe3Al also showed a similar densification behavior, and the microstructure of hot-pressed Fe3Al is shown in Figure 6. Hot-pressing of elemental powders of iron and aluminum resulted in a single-phase Fe3Al.

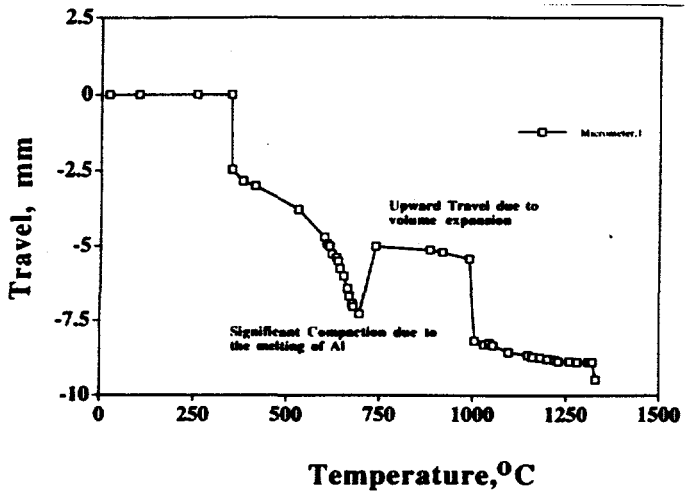

Figure 2 - Ram travel during hot-pressing of nickel-aluminide compsites.

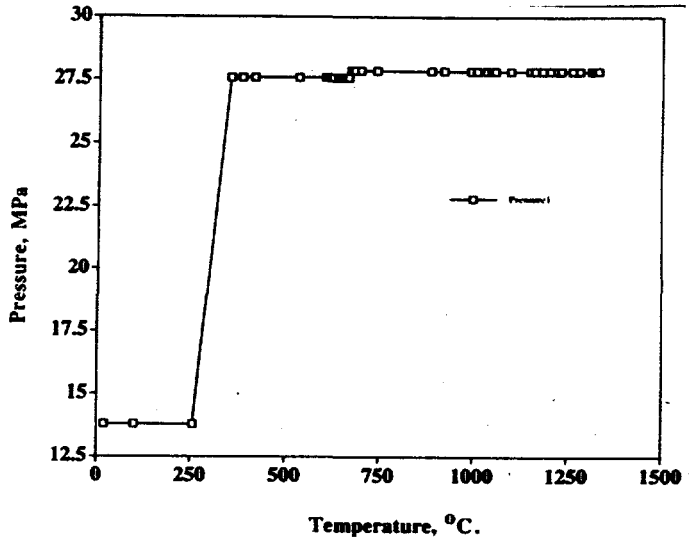

Figure 3 - Pressure versus temperature plot during hot-pressing of nickel-aluminide composites.

Table II. Densities of intermetallics obtained by reaction synthesis

Sample	Processing conditions	Percent theoretical maximum density
Ni_3Al[a]	Hot-processing of powders in vacuum	98.64
Ni_3Al[a] + 3.56 vol % Al_2O_3	Hot-pressing of powders in vacuum	99.08
Ni_3Al[a] + 6.88 vol % Al_2O_3	Hot-pressing of powders in vacuum	98.7
Fe_3Al	Hot-processing of powders in vacuum	98.2

[a]Comparison of Ni_3Al corresponds to nickel 77.92%, aluminum 21.73%, boron 0.01%, and zirconium 0.34% (all in atomic percent).

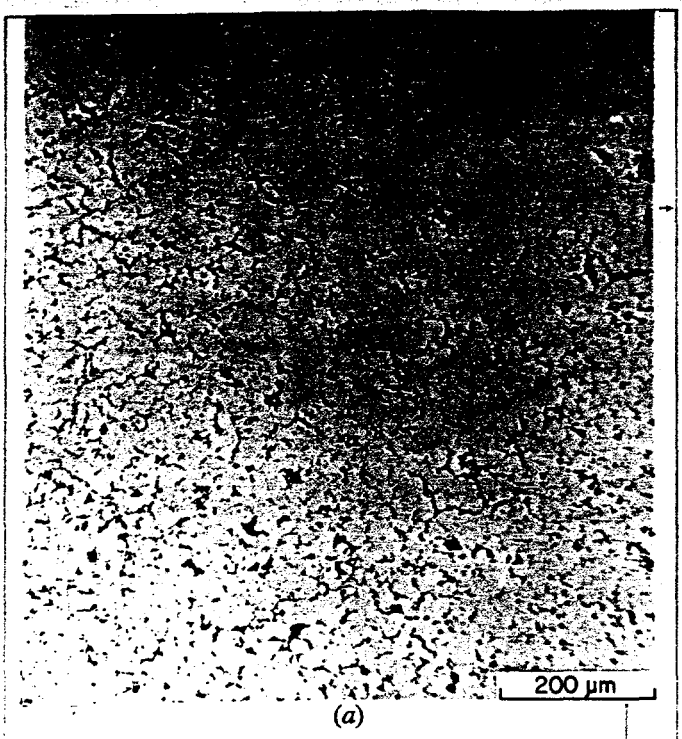

(a)

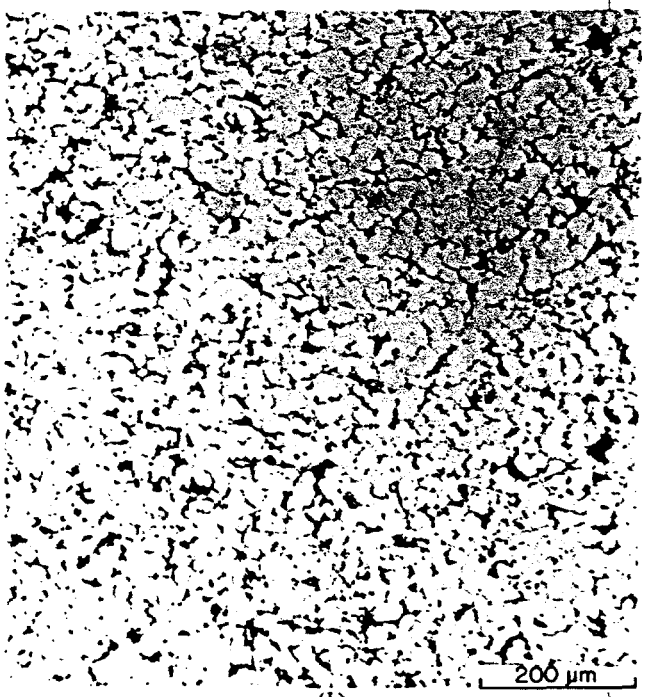

(b)

Figure 4 - Optical microstructures of Ni_3Al composites obtained by hot-pressing of 3Ni+Al with: (*a*) 2 wt % Al_2O_3 and (*b*) 4 wt % Al_2O_3.

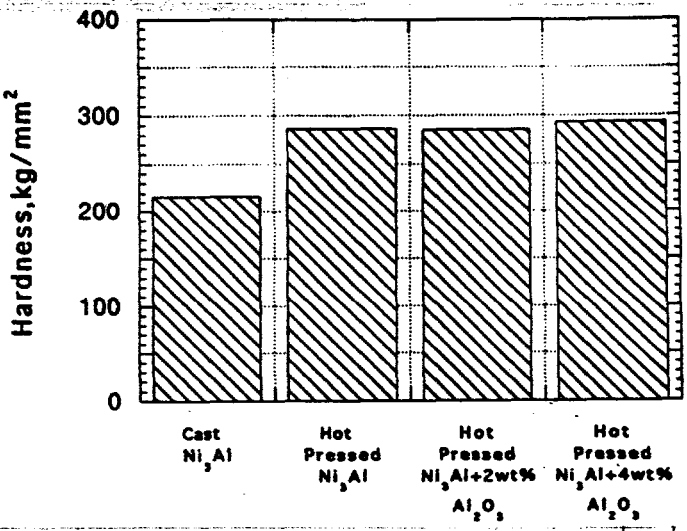

Figure 5 - A comparison of Vickers microhardnesses of cast Ni_3Al with hot-pressed Ni_3Al, and composites of Ni_3Al.

Figure 6 - Optical microstructure of Fe_3Al obtained by hot-pressing of iron and aluminum powders.

Text must not extend below this line.

Seetharama C.Deevi
AUTHOR

Table III compares mechanical properties of intermetallics obtained in as-pressed condition using button-head specimens at a strain rate of 4.572 mm/min with the published data. The strengths of the materials show excellent agreement with the published reports on cast Ni_3Al and hot-isostatically pressed materials. The tensile elongations of the hot-pressed materials are lower, and the lower elongations could be attributed either to the inhomogeneous mixing of boron or segregation of boron. It has been shown by Liu et al. (19) that the proper concentration of boron is essential in Ni_3Al to obtain good room-temperature tensile elongations. The strengths of materials compare well with earlier work carried out by experimental techniques such as reactive annealing, reactive infiltration, reactive sintering and reactive hot-isostatic pressing (see Table III).

Intermetallics based on FeAl were also obtained by hot-pressing of elemental powders with composition corresponding to Fe-24 Al with boron of 0.005, zirconium of 0.2, carbon of 0.06, and molybdenum of 0.42 wt % (identified as Fe-240). Ceramic phases such as TiC, ZrO_2, and Al_2O_3 were added to the base FeAl composition to determine the strengths of FeAl composites. Fine-grain sizes were observed in the case of hot-pressed FeAl intermetallic alloys and their composites, and the grain sizes were in the range of 15 μm. Figure 7 illustrates the microstructures of FeAl composites with 2 wt % TiC and 4 wt % Al_2O_3. Vickers microhardnesses of the composites shown in Figure 8 indicate that the hardnesses of the composites can be increased with the addition of ceramic phase.

The mechanical properties of FeAl and their composites were obtained from room temperature to 800°C in air. The yield strengths of FeAl and its composites are comparable, and the strength drops slowly until 600°C and falls abruptly between 600 to 800°C [see Figure 9(*a*)]. Ultimate tensile strengths indeed show the beneficial advantage of the addition of ceramic phase, and the tensile strength of FeAl alloy is lower than the tensile strengths of alumina-reinforced FeAl alloy [see Figure 9(*b*)]. It is important to note that the room-temperature tensile strengths approach 850 MPa, and the strength of FeAl even at 700°C is close to 500 MPa. Tensile elongations of FeAl and their composites are shown in Figure 9(*c*).

Figure 10(*a*) provides a comparison of yield strengths of FeAl alloys based on Fe-240 obtained by hot-pressing of elemental powders, air-induction melting (AIM), vacuum-induction melting (VIM), and the properties of FA-385 obtained by hot-extrusion of water-atomized FeAl alloy with and without boron (28). It is clear from Figure 10 that hot-pressed FeAl from elemental powders exhibits the best strength from room temperature to 700°C as compared to FeAl alloys made by extrusion and casting techniques. Figure 10(*a*) also clearly shows the superior strengths of FeAl alloys over steel. Figure 10(*b*) shows the tensile elongations of FeAl alloys.

Table III. Tensile properties of intermetallic powders consolidated using a hot press

Sample	Test temp. (°C)	Yield strength (MPa)	Tensile strength (MPa)	Total elongation (%)
Ni_3Al[a]	23	401	401	0.33
Ni_3Al[a] + 2 wt % Al_2O_3[a]	23	521	625	4.74
Ni_3Al[a] + 4 wt % Al_2O_3[a]	23	486	486	0.93
Fe_3Al[a]	23	404	521	0.30
Ni_3Al + B[b] (as HIP, 800°C)	25	286	--	14.8
Ni_3Al + B[b] (as HIP, 1100°C)	25	494	--	2.1
Ni_3Al + B[b] (heat treat, 1100°C HIP)	25	591	--	5.2
Ni_3Al + 3 vol % Al_2O_3 fiber (as HIP, 800°C)	25	474	--	1.0
Ni_3Al[c] (800°C HIP, 104 MPa, 30 min)	--	--	363	--
Ni_3Al + 0.1 wt % B[c] (800°C HIP, 104 MPa, 30 min)	--	265	722	10.0
Ni_3Al + 0.1 wt % B[c] (800°C HIP, 172 MPa, 60 min)	--	494	677	2.0
Ni_3Al[c] (reactive infiltration)	--	--	400	--

[a]Strain rate = 4.572 mm/min.

[b]Source: B. Moore, A. Bose, R. German, and N. S. Stoloff, Materials Research Society symposium proceedings, Vol. 120, p. 54 (1988).

[c]Source: D. C. Dunand, *Materials and Manufacturing Processes*, **10**(3), 373-403 (1995).

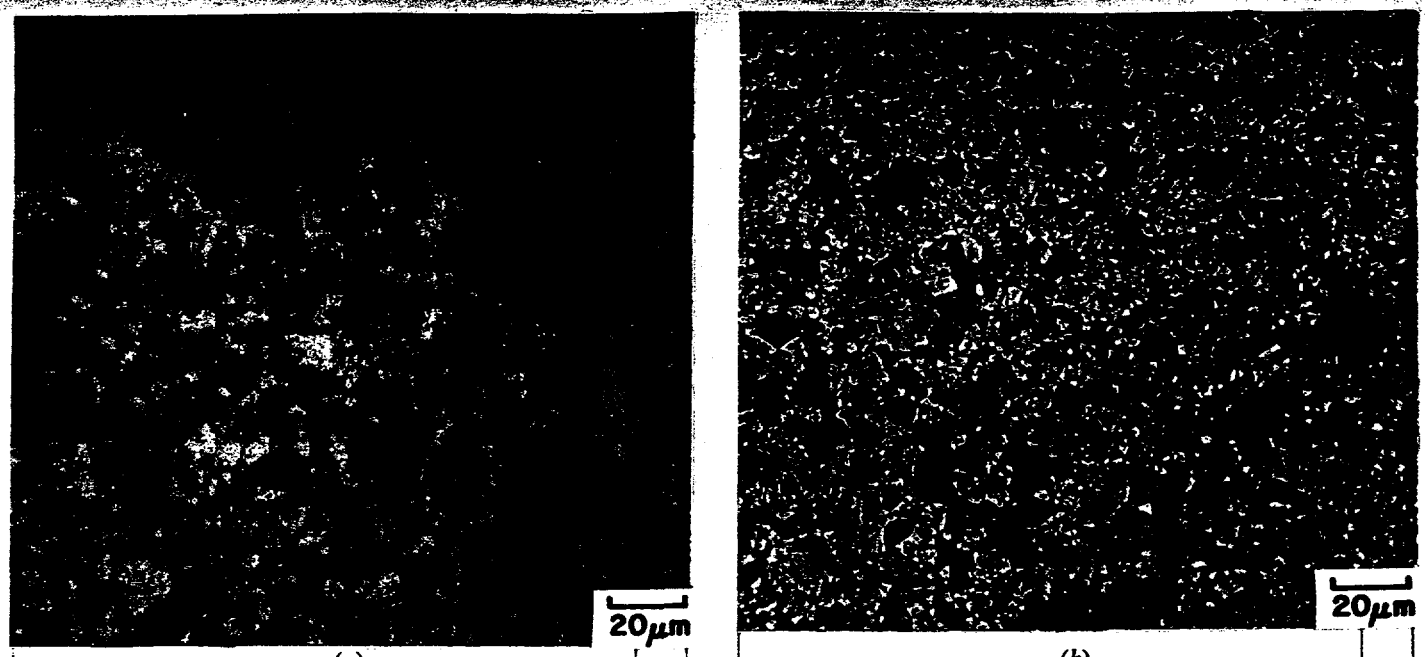

(*a*) (*b*)

Figure 7 - Optical microstructures of FeAl composites with (*a*) 2 wt % TiC and (*b*) 4 wt % Al_2O_3. Hot-pressing was carried out in vacuum at 1200°C in vacuum. Etchant used consisted of 40 ml HCl plus 10 ml HNO_3.

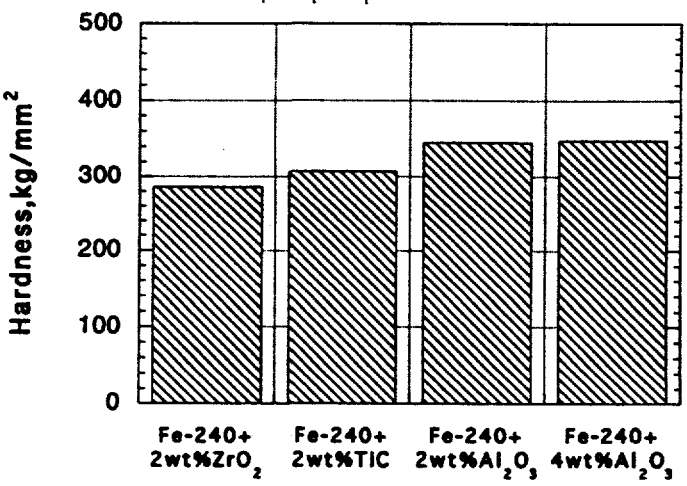

Figure 8 - Vickers microhardnesses of hot-pressed FeAl composites.

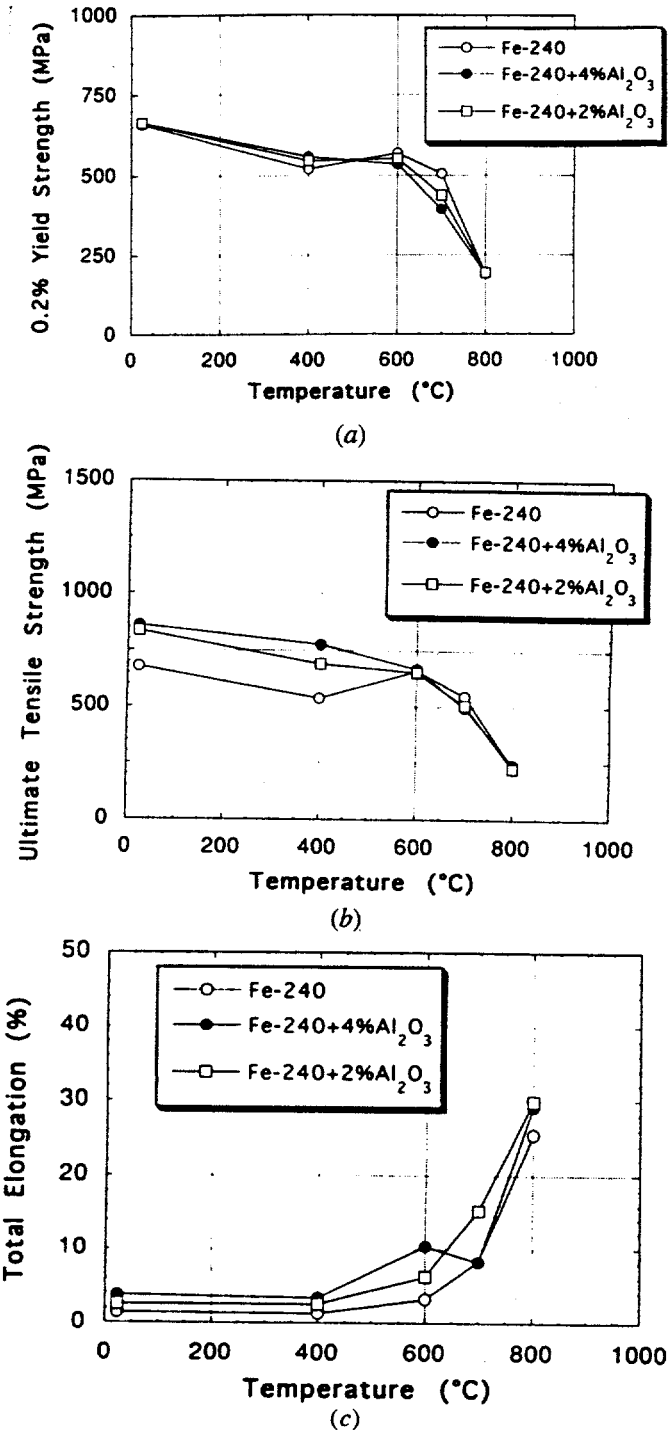

Figure 9 - Mechanical properties of FeAl alloy and FeAl composites with alumina: (*a*) yield strengths, (*b*) ultimate tensile strengths, and (*c*) tensile elongations.

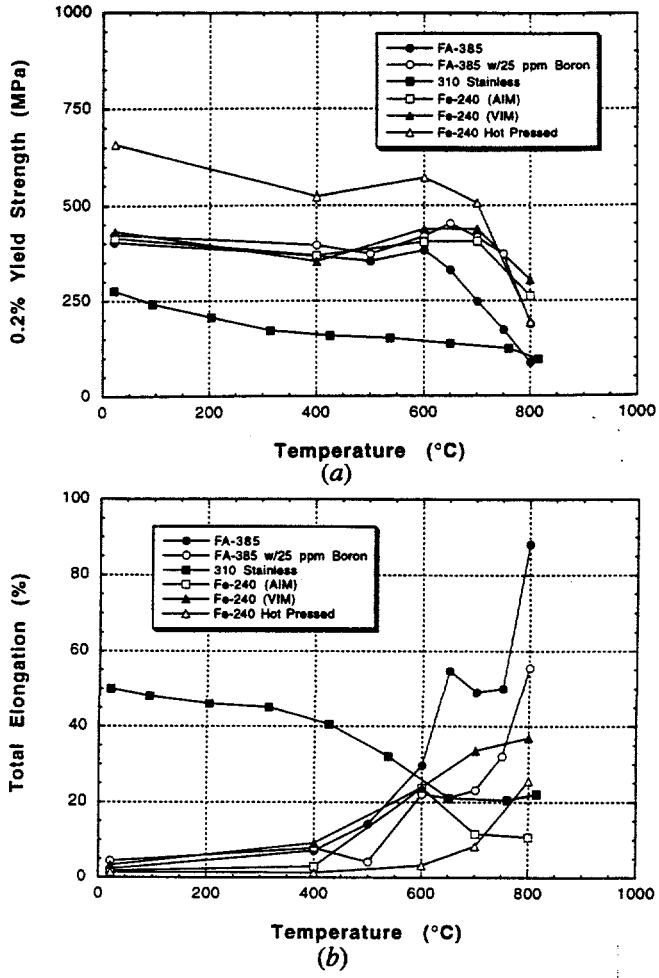

Figure 10 - A comparison of (*a*) yield strengths and (*b*) tensile elongations of FeAl alloys with steel.

Hot Extrusion

This technique is ideal for producing long bars, rods, and sheets of material with uniform cross section over a large length. Extrusion is generally carried out at high temperature, high-strain rate and high stress. Unlike hot-pressing, hot-extrusion would subject the particles to high-shear deformation which would ensure break-up of oxides present on the surfaces of the particles. In addition, hot-extrusion collapses pores and generates a high number of particle-particle contacts.

Figure 11 shows schematics of (*a*) hot-extrusion process and (*b*) hot-extrusion unit used to obtain FeAl powders. The extrusion was carried out using a hydraulic press. The pressure was transmitted to a stem which, in turn, transmitted the pressure to a penetrator, which is generally a dummy block. The penetrator transferred the pressure to the workpiece (a sealed container in most cases). A graphite block was placed between the dummy block and the sealed can to prevent back extrusion and also seal the end part of the can. The extrusion of a powder into full dense material is given by the flowing equation:

$$F = C A \ln (R) , \qquad (3)$$

where

F = the extrusion force is related to a constant, C, and is necessary to initiate extrusion of fine particles is generally higher than the force necessary to maintain the extrusion process;

C = a constant which is a measure of the difficulty in achieving deformation and flow of the powder and combines a variety of parameters such as flow stress, friction, and redundant work;

A = the cross-sectional area of the material;

R = the reduction ratio which is defined as the ratio of the cross-sectional areas before and after the reduction.

To determine whether exothermic reactions can be inititated during extrusion of aluminum cans containing intermetallic powders, elemental powders corresponding to Ni_3Al, NiAl, and Fe_3Al were packed in aluminum containers of 5.04 cm diam and extruded at different preheating temperatures. Containers were evacuated by heating the cans at 150°C for at least 6 h prior to sealing the cans. As can be noted from Table IV, extrusion of elemental powders with reduction ratios of 1:20, 1:16, and 1:12 initiated exothermic diffusional reactions between aluminum and nickel and aluminum and iron powders due to the frictional heating associated with the extrusion. Frictional heating associated with the initial reduction of the surface areas of the can allowed melting of aluminum, which, in turn, triggered the exothermic reaction. The heat generated by the reaction melted the aluminum can and also oxidized the aluminum and the product (27).

Since frictional heating and the exothermicity of the reaction melted the aluminum cans, blended powder mixtures of Fe-24% Al were evacuated and sealed in steel cans. The sealed cans were preheated by placing them in a box furnace at 450°C for 1 h to initiate solid-state reactions, and in another box furnace for 1 h at 900°C to form the desired intermetallics. This was done to ensure that initial reactions at 450°C were controlled solid-state reactions leading to partial reaction and secondary products, and the heating at 900°C was carried out to ensure completion of the reaction by utilizing the thermal explosion mode of combustion synthesis. An extrusion temperature in the range of 950 of 1200°C and a reduction ratio of 16:1 for extrusion of steel cans were used to obtain dense intermetallic bar encased in steel. The extruded rods were machined to obtain samples for tensile testing, microhardness, and microstructural evolution.

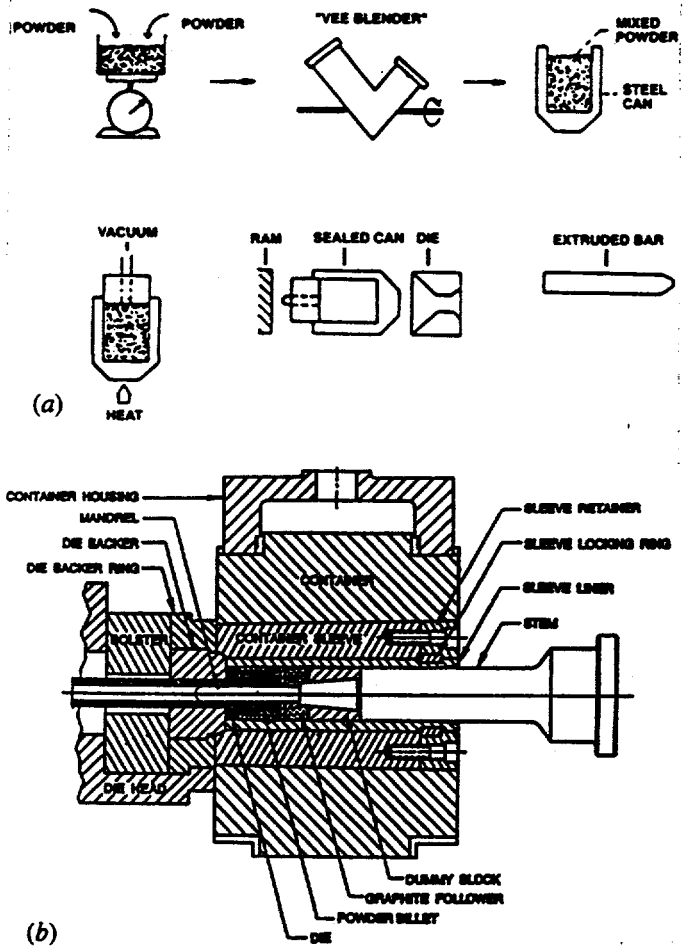

Figure 11 - Schematic diagrams of (*a*) extrusion process and (*b*) extrusion press used at the Oak Ridge National Laboratory to extrude elemental powders in sealed cans.

Figure 12 shows the microstructural features of FeAl extruded at 950°C in the longitudinal direction at 200 and 1000×. Long streaks of FeAl can be seen at a low magnification of 200×, and the grain structure of FeAl is visible at a high magnification of 1000×. Figure 13 shows the microstructural features in the transverse direction near the center of the extrusion. Microstructures shown in both the longitudinal and transverse directions indicate a uniform and fine-grain-size microstrcture. Grain sizes exhibited a small increase with increase of extrusion temperature, and all of the samples showed a single-phase FeAl by X-ray diffraction technique.

Table IV. Extrusion conditions and characteristics of extrusion of intermetallic powders

Experiment no.	Elemental composition to obtain	Temperature of the material	Liner temperature of extrusion press (°C)	Pressure (tons)	Reduction ratio	Observations
4082 (Al can)	NiAl	425°C, 1 h	425	310	20:1	Extruded well, reacted fully, and melted aluminum can
4083	Ni_3Al (Al can)	425°C, 1 h	425	262	20:1	Extruded well, reacted fully, and melted aluminum can
4084	*a*	RT[a]	425	310	20:1	Did not extrude
4085	Fe_3Al compact (Al can)	425°C, 1 h	425	295	10:1	Extruded well, reacted fully, and melted aluminum can
4086	Ni Al compact (Al can)	425°C, 1 h	425	280	12:1	Extruded well, reacted fully, and melted aluminum can
4087	*a*	RT[b]	425	300	12:1	Extruded well and fully reacted
4088	Ni_3Al (Al can)	RT[b]	425	310	12:1	Extruded well, reacted fully, and partially melted aluminum can
4089	NiAl (Al can)	RT[b]	425	290	8:1	Extruded but no reaction
4090	Ni_3Al	RT[b]	425	300	8:1	Extruded well but no reaction

[a]IC-50 (CIPed) = Ni 77.92%, Al 21.73%, B 0.01%, and Zr 0.34% (in atomic percent).
[b]RT = room temperature.

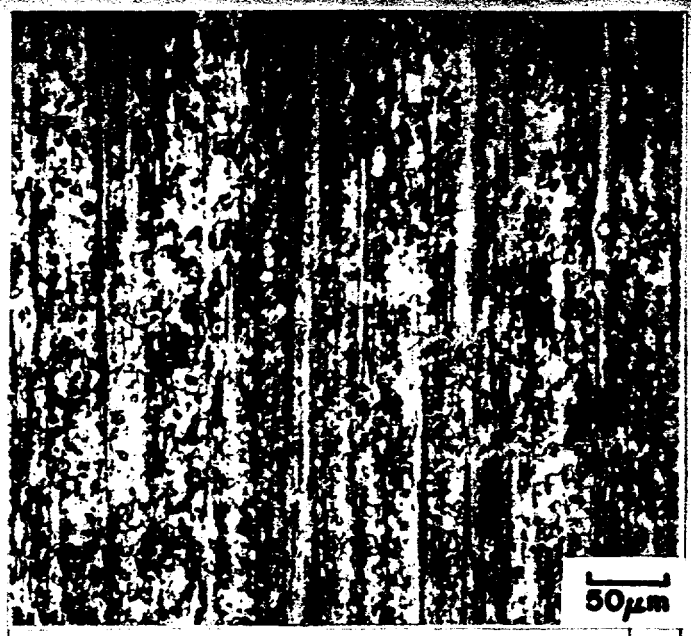

(*a*)

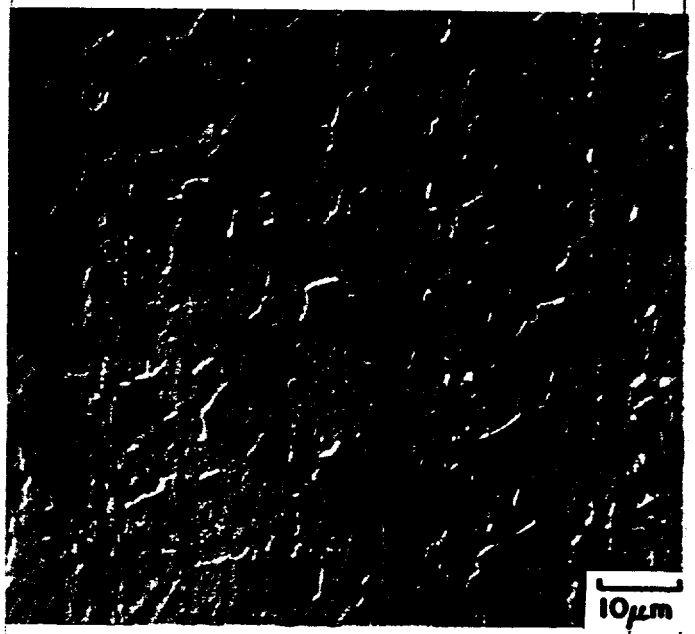

(*b*)

Figure 12 - Optical microstructure of FeAl extruded at 950°C from Fe-24 wt % Al elemental powders; longitudinal direction near center; etched with Keller's agent: (*a*) 200× and (*b*) 1000×.

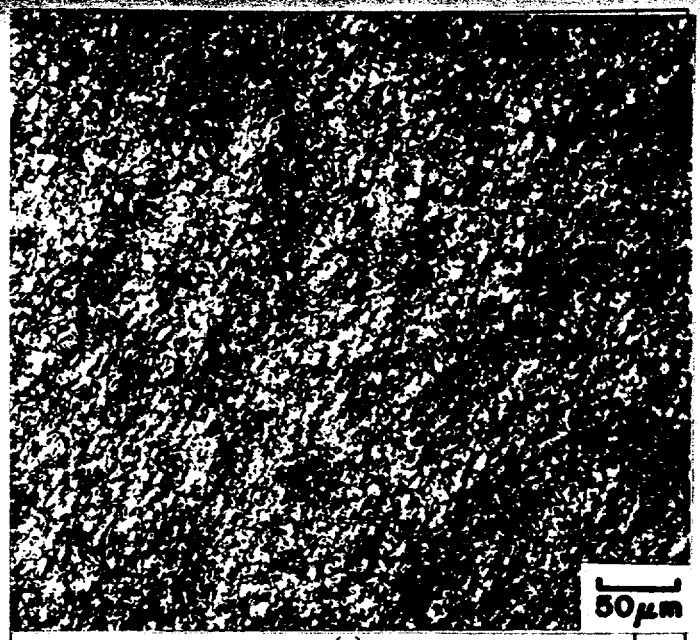

(*a*)

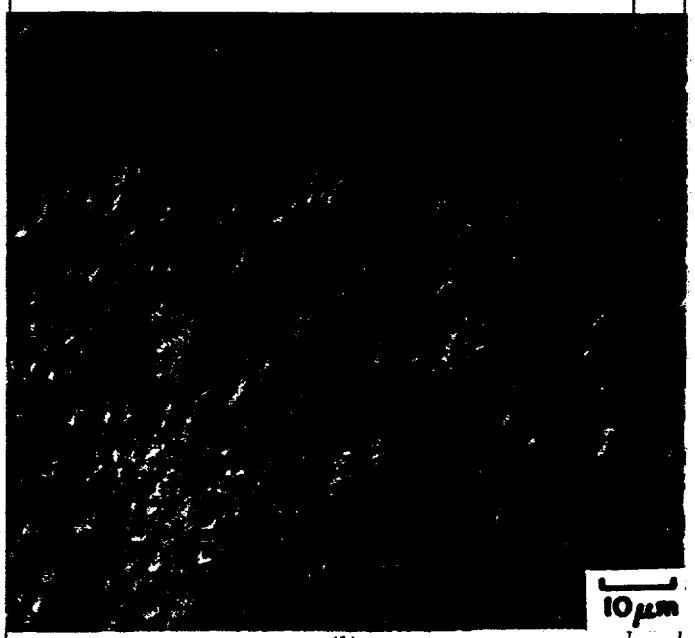

(*b*)

Figure 13 - Optical microstructure of FeAl extruded at 950°C from Fe-24 wt % Al elemental powders; transverse direction near center; etched with Keller's agent: (*a*) 200× and (*b*) 1000×.

Text must not extend below this line.

Seetharama C. Deevi
AUTHOR

Tensile properties of extruded FeAl alloys were determined from room temperature to 800°C in air. Yield strengths, ultimate tensile strengths, and tensile elongations indicate that a low-extrusion temperature will provide a high-strength material. While the yield strength of FeAl extruded at 950°C indicated a sharp decline above 400°C, the FeAl extruded at 1100°C remained constant until 600°C before it declined with temperature. Figure 14 shows the yield strenghs and tensile elongations of FeAl extruded at 950, 1000, and 1100°C.

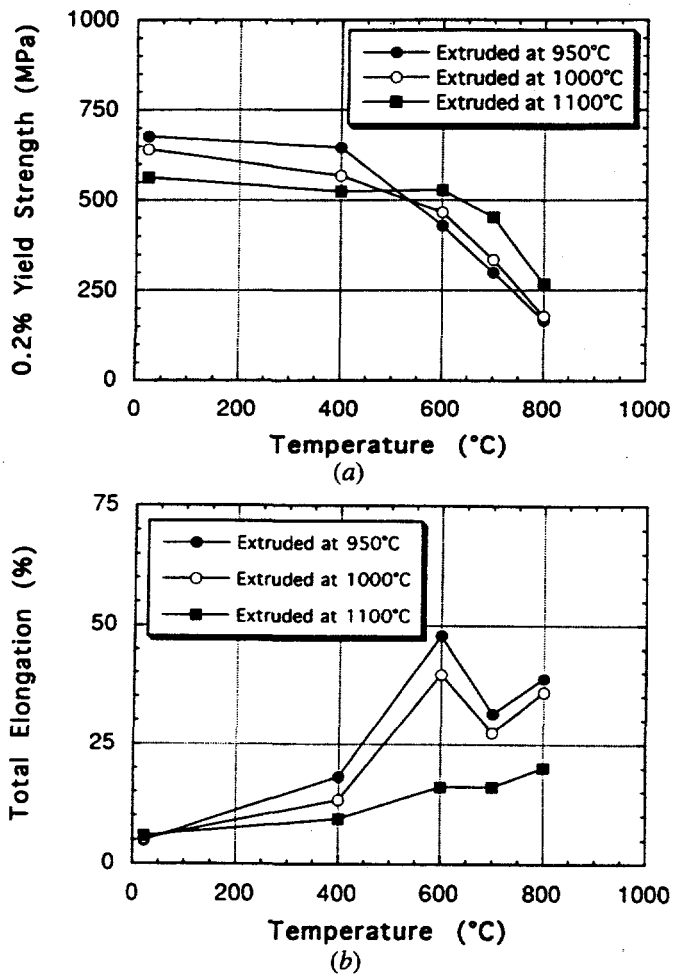

Figure 14 - (*a*) Yield strengths and (*b*) tensile elongations of Fe-24 wt % Al extruded at 950, 1000, and 1100°C in a steel can using elemental powders of iron and aluminum powders.

Processing of Fe- 8 wt % Al Alloy by Combustion Synthesis

In order to show that combustion synthesis can be combined with conventional metal-working processes, Fe-8 Al-1 Mo-0.12 Ti-0.42 Zr -0.5 Y (all in weight percent) were mechanically alloyed in an attritor for 8 h in argon. The powder was cold-isostatically pressed into a cylindrical compact of 5 cm diam, and the compact was ignited in air to propagate the combustion wave. After a prolonged period of heating on the surface, the compact ignited and the wave propagated through the compact. The compact was hot-forged and rolled in a stainless steel cover at 1100°C. A schematic of the processing scheme is shown in Figure 15.

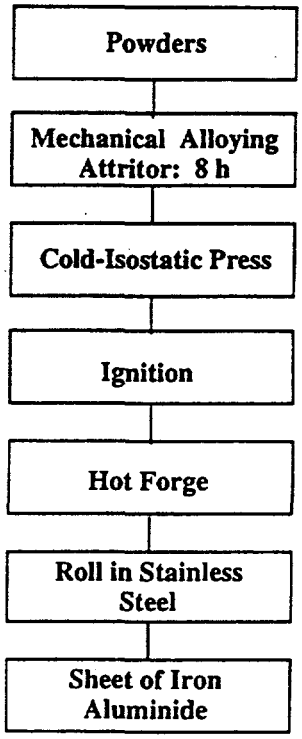

Figure 15 - Alloy Fe-8 Al-1 Mo-0.12 Ti-0.42 Zr-0.50 Y prepared by combustion synthesis and processing.

A rolled sheet measuring 0.75 mm was used to determine the tensile properties from room temperature to 800°C. As can be noted from Figure 16, the yield strenghs of Fe-8 wt % Al obtained by combustion synthesis are slightly higher than the mechanically alloyed FeCrAlY (commercially available from INCO Alloys under the trade name MA-956), and the allloys (FAS, FAL and FA-129) developed at ORNL. The compositions of FAS, FAL, and FA-129 are shown in Table V. The high strength of the combustion-synthesized alloy can be attributed to the oxide-dispersion strengthening due to the oxidation of the elemental powders in air. Surprisingly, the oxide strengthening can primarly be attributed to the oxidation of zirconium.

Reactive Spraying of Nickel and Iron Aluminides

The heats of formation of intermetallics (see Table I) can be utilized in thermal-spray coatings by feeding elemental powders or unalloyed material such that an exothermic reaction can be favored either before or after the elemental powders are deposited on a substrate. This can be accomplished by controlling the velocity, power, and plasma-torch design. Plasma transfers intense heat to the feed material as it passes

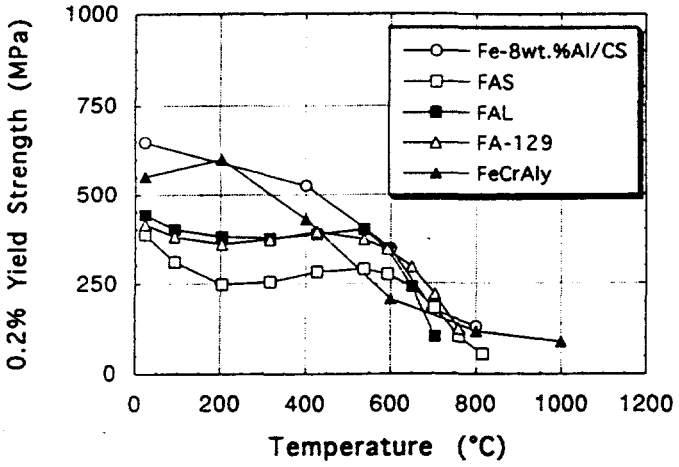

Figure 16 - Comparison of yield strengths of combustion-synthesized Fe-8 wt % Al alloy with FAS, FAL, FA-129, and FeCrAlY.

through the torch, and the heat transfer is generally sufficient to bring the particles to a molten state. Molten-metal particles may react in the plasma before or after deposition on a substrate. A variety of coating techniques such as plasma spraying, vacuum-plasma spraying, flame spraying, and arc spraying fall broadly under the category of thermal-spray techniques. Therefore, thermal-spray technology offers another avenue to apply the principles of combustion synthesis or reaction synthesis for surface modification or to produce in-situ intermetallic coatings on the substrate.

Several experiments were carried out by feeding nickel and aluminum and iron and aluminum powders through a dc plasma torch. X-ray diffraction analysis of the coatings revealed that the plasma spraying of nickel and aluminum resulted in product phases such as $NiAl_3$ and Ni_5Al_3 along with elemental powders of nickel and aluminum. In some cases, annealing of the coating was required to homogenize and stabilize the microstructure and obtain a desired intermetallic phase. Table VI provides a summary of the experimental conditions and the observed product phases (29). Similar results were obtained with the Fe-Al system (30).

Extension of Reaction Synthesis Principles to Exo-Melt™ Process

Reaction-synthesis principles were also applied to the melting and casting of intermetallics (15-18) by modifying the loading sequence of melt stock. The total melt stock of nickel was divided into two parts. One part contained nickel in a ratio proportional to NiAl while the remaining part of the nickel was loaded at the bottom. All of the alloying elements were loaded on top of the nickel. The aluminum melt stock was located vertically on top of the alloying elements, and the rest of the nickel (corresponding to NiAl) was loaded on top of the alloying elements. Aluminum was placed around the crucible so that the molten aluminum would react with the nickel and form NiAl on top such that the reaction with a high-combustion temperature would form initially. The aluminum-loading sequence was designed to preferentially form NiAl on top of the melt stock as opposed to Ni_3Al. Thermodynamically, formation of NiAl is preferred over Ni_3Al since NiAl formation releases –14.15 kcal/g atom with a temperature of 1639°C, whereas Ni_3Al formation is accompanied by only about –9.15 kcal/g atom with a temperature of 1270°C.

A plot of time versus temperature during melting of IC-221M by the Exo-Melt™ process is shown in Figure 17. The temperatures monitored by all three thermocouples indicated an increase with time, and a linear rate of heating was seen with the thermocouple located in the alloying elements. The thermocouple placed in the aluminum melt stock indicated a sudden temperature drop and remained constant for a few minutes. A sudden rise in temperature by about 400°C can be seen from a thermocouple located in the nickel melt stock while the temperature of alloying elements increased almost linearly with time. This temperature increase at a time of 6.5 min can be attributed to the temperature rise associated with molten NiAl dripping from the top onto the nickel. Several dips associated with the melting of aluminum can be seen from the thermocouple located in the aluminum melt stock, while the temperature of alloying elements increased linearly with time (see Figure 17).

It can be seen from Figure 17 that the entire melting process was completed within 12 min, while melting of Ni_3Al by conventional melting would take at least 30 min. Some of the positive attributes of the Exo-Melt™ process are given in ref. 15.

Composites Based on Thermite Reactions

It is well known that heat released in thermite reactions is much higher than in combustion synthesis of materials such as Ni_3Al, NiAl, Fe_3Al, FeAl, and $MoSi_2$ due to the oxidation of metal as shown in Eq. (4) below.

$$Fe_2O_3 + Al \rightarrow Fe + Al_2O_3 \qquad (4)$$

Composites based on thermite reactions can be moderated by the addition of a diluent as discussed in (5) or by ensuring that the reactions take place in a controlled manner. To obtain an in-situ synthesized FeAl composite with Al_2O_3, a thermite mixture based on Fe_2O_3 + Al was added at 5, 10, 15, 20, and 30 wt % to an elemental powdered mixture of iron and aluminum (1:1 at. %) intermetallic. Composites were obtained by extruding the preblended mixtures at 1100°C. Figure 18 shows uniform dispersion of fine alumina throughout the matrix of intermetallic. Reaction-synthesis experiments were also carried out using Ceracon's process at 1100°C (ref. 30) by V-blending 5, 10, and 20 wt % of the preblended thermite mixture to a blended mixture of iron and aluminum (1:1 at. %). Figure 19 shows the microhardnesses of iron aluminide FeAl with 5% thermite mixture by Ceracon's process, FAL and FA-386M1. As can be noted from the

Table V. Compositions of Fe_3Al-based alloys developed for commercial applications and compositions of some commercial alloys

Element	Alloy (weight percent)						
	FAS[a]	FAL[b]	FA-129[c]	FAH	Fecralloy	MA-956	Type 310
Al	15.9	15.9	15.9	15.9	4.5	--	--
Cr	2.20	5.5	5.5	5.5	16.0	20.0	25.0
B	0.01	0.01	--	0.04	--	--	--
Zr	--	0.15	--	0.15	--	--	--
Nb	--	--	1.0	1.04	--	--	--
C	--	--	0.05	--	0.02	--	0.15
Mo	--	--	--	1.00	--	--	--
Si	--	--	--	--	--	--	0.50
Y	--	--	--	--	0.3	--	--
Y_2O_3	--	--	--	--	--	0.5	--
Ti	--	--	--	--	--	0.5	--
Ni	--	--	--	--	--	--	20.0
Fe	*d*	*d*	*d*	*d*	*d*	*d*	*d*

[a]Sulfidation-resistant alloy.
[b]High room-temperature (RT) tensile ductility.
[c]High-temperature strength with good RT ductility.
[d]Balance.

Table VI. Observed phases in selected plasma-sprayed coatings obtained on carbon steel substrates

Sample no.	Target Ni/Al ratio (wt %)	Method of mixing	Power (kW)	Velocity	Preheat or postspray annealing	Average coating thickness (mm)	Observed phases[a]
32395-32	87:13	Blended	40	Subsonic	–	0.225	Ni^{vs}, Al_3Ni^{s}, Al^{w}, $Al_3Ni_2^{vw}$
32395-32	87:13	Blended	40	Subsonic	Postspray 1 h, 600°C 1 h, 800°C 1 h, 1100°C furnace cool	0.225	Ni^{vs}, $AlNi_3^{s}$, Al_3Ni^{w}, Al^{vw}
32395-4	87:13	Blended	44	Mach I	–	0.200	Ni^{vs}, Al^{s}, Al_3Ni^{w}, $Ni_5Al_3^{vw}$
32395-4	86:14	Blended	44	Mach I	Postspray 1 h, 600°C 1 h, 800°C 1 h, 1100°C furnace cool	0.200	$NiAl_3^{vs}$, Al^{s}
41895-12	1:1	Dual fed	45	Subsonic	–	0.775	Ni^{vs}, Al_3Ni^{s}, Al^{w}, $Ni_5Al_3^{vw}$, $Al_{0.42}Ni_{0.58}^{t}$
40795-9	80:20	Encapsulated powder	37	Subsonic	Preheat	0.150	Ni^{vs}, Al^{s}, $Al_3Ni_2^{t}$
40795-9	80:20	Encapsulated	37	Subsonic	100°C preheat postspray 1 h, 600°C 1 h, 800°C 1 h, 1100°C furnace cool	0.150	Ni^{vs}, $AlNi_3^{s}$, Al^{w}

[a] vs = very strong, s = strong, w = weak, vw = very weak, and t = trace.

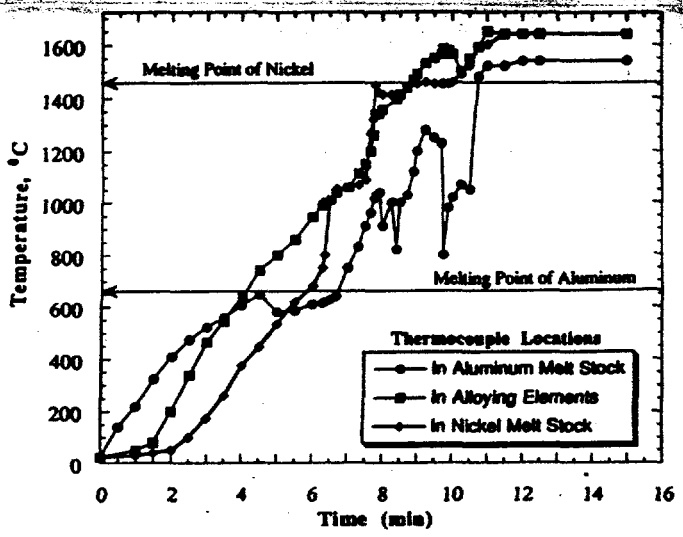

Figure 17 - A plot of time versus temperature obtained with three Pt—Pt/13% Rh thermocouples located in the melt stock of IC-221M (composition: Ni = 81.146, Al = 7.981, Zr = 1.697, Cr = 7.740, Mo = 1.428, and B = 0.008). Melting was carried out by the Exo-Melt™ process.

iron aluminide composite obtained by the addition of a thermit mixture exhibits high hardness, and the hot hardness of the composite is higher than FeAl and iron-based alloys. We are presently evaluating the tensile and compressive properties of the composites.

Summary and Conclusions

Intermetallics and intermetallic composites based on nickel and iron aluminides have been successfully produced by hot-pressing, hot-extrusion, and a combination of mechanical alloying and combustion synthesis by application of reaction-synthesis principles. Intermetallics obtained by reaction synthesis exhibited superior mechanical properties as compared to the materials obtained by melting and extrusion of prealloyed powders. The superior yield and tensile strengths can be attributed to the uniform microstructures and fine-grain sizes of the materials.

Reaction-synthesis principles were also extended to thermal spray techniques to obtain intermetallic coatings, and the results suggest that plasma spraying of elemental powders lead to intermetallic phases with high-aluminum content. A step-wise annealing was found to be necessary to achieve the desired intermetallic.

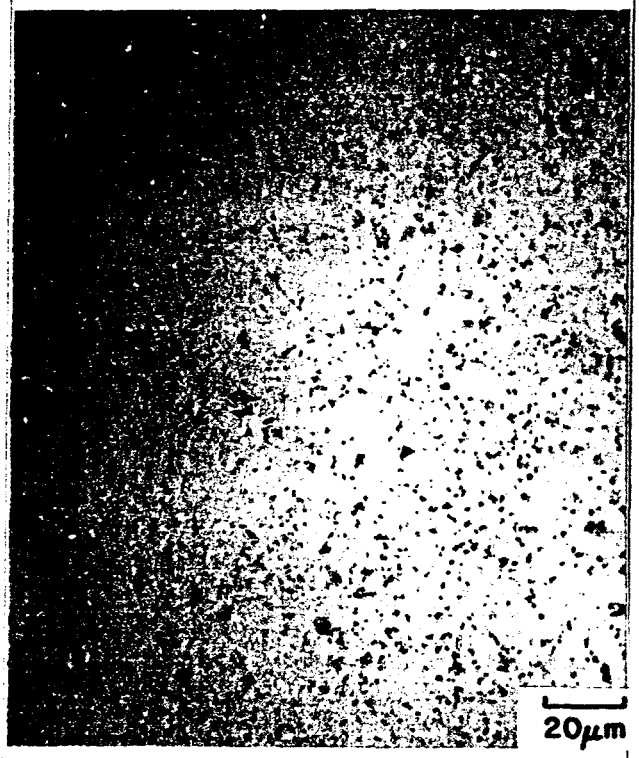

(a)

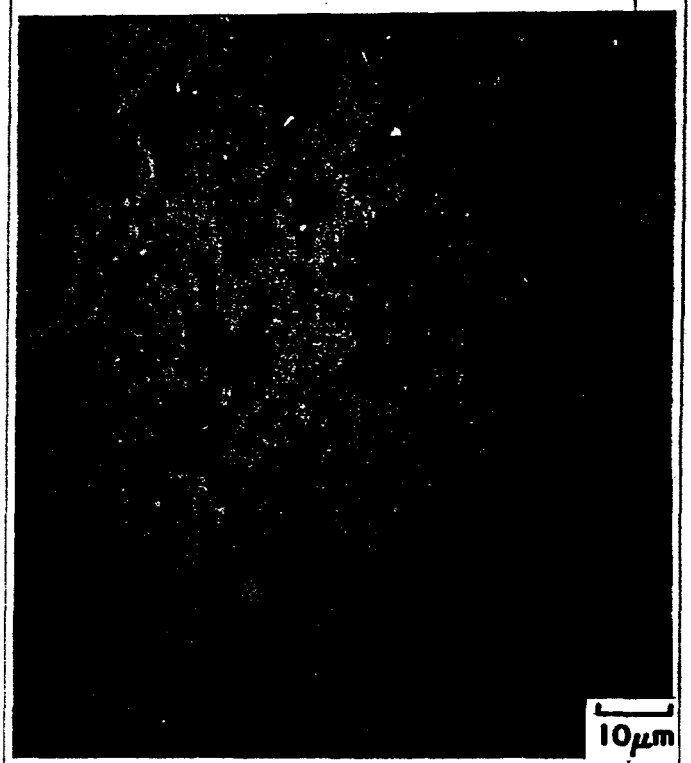

(b)

Figure 18 - Microstructure of iron plus aluminum with 10 wt % of Fe_2O_3 + Al mixture extruded at 1100°C in mild steel can indicates dispersion of Al2O3 in iron aluminide: (*a*) as-polished condition at 500×, and (*b*) condition after etching at 1000×.

Seetharama C. Deevi
AUTHOR

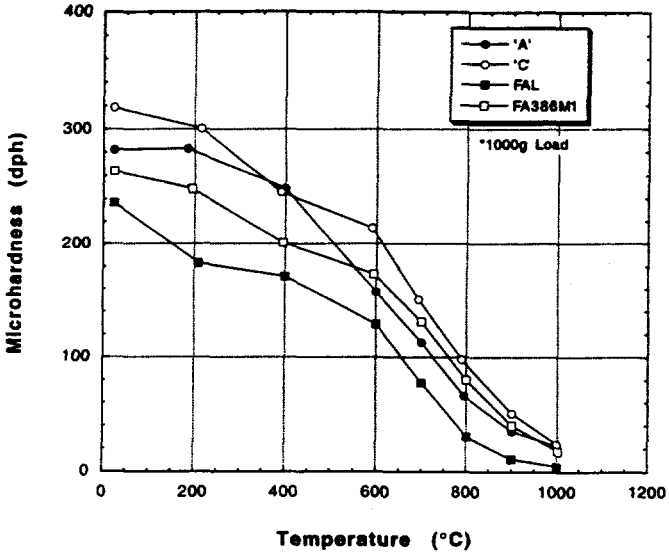

Figure 19 - Comparison of hardness as a function of test temperature for iron-aluminide alloys.

Acknowledgments

The authors thank K. S. Blakely, E. C. Hatfield, and C. R. Howell for experimental work; E. K. Ohriner and C. A. Blue for paper review; and M. L. Atchley for manuscript preparation.

Research was sponsored by Philip Morris U.S.A. , the U.S. Department of Energy, Assistant Secretary for Energy Efficiency and Renewable Energy, Office of Industrial Technologies, Advanced Industrial Materials Program, and Office of Fossil Energy, Advanced Research and Technology Development Materials Program [DOE/FE AA 15 10 10 0, Work Breakdown Structure Element ORNL-2(H)] under contract DE-AC05-96OR22464 with Lockheed Martin Energy Research Corp.

References

1 Frankhouser, W.L., K.W. Brendley, M.C. Kieszek, and S.T. Sullivan, "Gasless Combustion Synthesis of Refractory Compounds," 10, Noyes Publications, Park Ridge, New Jersey (1985).

2 Yi, H.C. and J.J. Moore, J. Mater. Sci., 25, 1159-1168 (1990).

3 Rabin, B.H., R.N. Wright, J.R. Knibloe, R.V. Raman, and S.V. Rale, Mat. Sci. & Engg., A153, 706 (1992).

4 Munir, Z.A., Ceramic Bull., 67, 342-349 (1988).

5 Munir, Z.A. and V. Anselmi-Tamburini, Mater Sci. Rep., 3, 277-365 (1989).

6 Deevi, S.C., J. Mater. Sci., 26, 2662 (1991).

7 Deevi, S.C., J. Mater. Sci., 26, 3343 (1991).

8 German, R.M., "Thermal Analysis in Metallurgy," 205-31, The Minerals, Metals & Materials Society, Warrendale, Pennsylvania (1992).

9 Philpot, K.A., Z.A. Munir, and J.B. Holt, J. Mater. Sci. 22, 159-69 (1987).

10 Naiborodenko, Y.S. and V.I. Itin, "Combust. Explos. Shock Waves," 11, 293-300 (1975).

11 Naiborodenko, Y.S. and V.I. Itin, Combust. Explos. Shock Waves, 11, 626-29 (1975).

12 Wang, L.L., Z.A. Munir, and Y.M. Maximov, J. Mat. Sci., 28, 3693 (1993).

13 Deevi, S.C., "Covalent Ceramics II: Non-Oxides," 171-76, Materials Research Society, Pittsburgh, Pennsylvania (1994).

14 Feng, H.J., J.J. Moore, and D.G. Wirth, Met. Trans., 23A, 2373 (1992).

15 Deevi, S.C. and V.K. Sikka, J. Intermetallics, 4, 357-375 (1996).

16 Deevi, S.C. and V.K. Sikka, J. Intermetallics (in press).

17 Sikka, V.K., S.C. Deevi, and J.D. Vought, Adv. Mater. Process., 147, 29-31 (1995).

18 Orth, J.E. and V.K. Sikka, Adv. Mater. Process., 148, 33-34 (1995).

19 Liu, C.T., "Structural Intermetallics," 365, The Minerals, Metals & Materials Society, Warrendale, Pennsylvania (1993).

20 Koch, C.C., C.T. Liu, and N.S. Stoloff, "High Temperature Ordered Intermetallic Alloys," Vol. 39, 560, Materials Research Society, Pittsburgh, Pennsylvania (1985).

21 Whang, S.H., C.T. Liu, D.P. Pope, and J.O. Stiegler, "High Temperature Aluminides and Intermetallics,"593, The Minerals, Metals and Materials Society, Warrendale, Pennsylvania (1990).

22 Liu, C.T., R.W. Cahn, and G. Sauthoff, "Ordered Intermetallics — Physical Metallurgy and Mechanical Behavior," 101, Kluwer Academic Publishers, Dordrecht, The Netherlands (1992).

23 Tortorelli, P.F. and J. H. DeVan, "Processing, Properties, and Applications of Iron Aluminides," 257, The Minerals, Metals and Materials Society, Warrendale, Pennsylvania (1994).

24 McKamey, C.G., J.H. DeVan, P.F. Tortorelli, and V.K. Sikka, J. Mater. Res., 6(8), 1779 (1991).

25 Stoloff, N.S., D. Alven, and C.G. McKamey, "An Overview of Fe3Al Alloy Development with Emphasis on Creep and Fatigue," ASM International, Materials Park, Ohio (to be published).

26 Maziasz, P.J., C.T. Liu, and G.M. Goodwin, "Proceedings of 2nd International Conference on Heat Resistant Materials," 555-566, ASM International, Cleveland, Ohio (1995).

27 Deevi, S.C. and V.K. Sikka, Mater. Res. Symp. Proc., 364, 917 (1995).

28 Maziasz, P.J., C.T. Liu, and G.M. Goodwin, "Proceedings of 2nd International Conference on Heat Resistant Materials," 555-566 ASM International, Cleveland, Ohio (1995).

29 Deevi, S.C., V.K. Sikka, R.D. Seals, and C.J. Swindeman, J. Thermal Spray Technology (in press).

30 Deevi, S.C., R.D. Seals, V.K. Sikka, and C.J. Swindeman, J. Mat. Sci. (in press).